Structure of the $\Lambda(1405)$ resonance and the $\gamma p \to K^+ + (\pi\Sigma)^0$ reaction

S. Marri and M. N. Nasrabadi*
Faculty of Physics, University of Isfahan, 81746-73441, Isfahan, Iran

S. Z. Kalantari
Department of Physics, Isfahan University of Technology, Isfahan 84156-83111, Iran

(Received 29 January 2020; revised 9 March 2021; accepted 3 May 2021; published 24 May 2021)

Three-body calculations of the $K\bar{K}N$ system with quantum numbers $I = 1/2$, $J^\pi = (\frac{1}{2})^+$ were performed. Using separable potentials for two-body interactions, we calculated the $\pi\Sigma$ mass spectra for the $(\bar{K}N)_{I=0} + K^+ \to (\pi\Sigma)^0 K^+$ reaction on the basis of the three-body Alt-Grassberger-Sandhas equations in the momentum representation. In this regard, different types of $\bar{K}N$-$\pi\Sigma$ potentials based on a phenomenological and chiral SU(3) approach were used. The possibility to observe the trace of the $\Lambda(1405)$ resonance in the $(\pi\Sigma)^0$ mass spectrum was studied. Using the χ^2 fitting, it was shown that the mass of the $\Lambda(1405)$ resonance is about 1417 MeV/c^2.

DOI: 10.1103/PhysRevC.103.055204

I. INTRODUCTION

An important problem in the strangeness sector of nuclear physics is the interaction of the antikaon and nucleon. The $I = 0$ channel of the $\bar{K}N$ interaction is dominated by the $\Lambda(1405)$ resonance, which is also a challenging issue in the strange nuclear physics. Because of the light mass of the $\Lambda(1405)$ resonance, it is difficult to describe it as a three-quark system in a constituent quark model. Therefore, the people usually take it as a quasibound state in the $\bar{K}N$ system. Dalitz and Tuan predicted the existence of the $\Lambda(1405)$ resonance using experimental data of the $\bar{K}N$ scattering length [1,2]. The experimental evidence of that was reported in 1961 in the $K^- p \to \pi\pi\pi\Sigma$ reaction [3]. The $\pi^+\Sigma^-$ mass spectrum in the $K^- d \to \pi^+\Sigma^- n$ reaction was studied by Braun *et al.,* and a resonance energy was found at 1420 MeV [4]. The $\pi^\pm\Sigma^\mp$ mass spectrum in the $\pi^- p \to K^+\pi\Sigma$ reaction was studied in Ref. [5] and a Λ mass of 1405 MeV/c^2 was deduced. In recent years, many efforts have been made to study the structure and nature of the $\Lambda(1405)$ resonance [6–19]. The theoretical studies based on chiral SU(3) dynamics for the $\bar{K}N$ interaction suggest a two-pole structure for $\Lambda(1405)$ [6–9,12,14], while the phenomenological models [10,11,13,17,18] suggest a one-pole structure.

In recent years the theoretical and experimental investigations have been pursued by different groups to study the nature and structure of the $\Lambda(1405)$ resonance [20–31]. In the last few years, a large number of data on the $\gamma p \to K^+(\pi\Sigma)$ reaction were reported by the CLAS collaboration at Jefferson Laboratory [20,21]. The $\pi\Sigma$ mass spectrum in different particle channels was determined in a wide energy range and with good resolution. For the first time, the quantum numbers of the $\Lambda(1405)$ resonance were determined based on experimental measurements [32]. The CLAS data together with the kaonic hydrogen data can be used as a benchmark of our analysis of the $\bar{K}N$ interaction. Several theoretical studies have been performed to analyze the CLAD data based on chiral SU(3) [33–37] and a phenomenological approach [38]. The CLAS data were analyzed in Refs. [33–37] using chiral dynamics, and a double-pole structure was predicted for the Λ resonance, while, in Ref. [38], a Λ mass of 1405 MeV was deduced from the same CLAS data.

The $\gamma p \to K^+(\pi\Sigma)^0$ reaction is depicted in Fig. 1. In this reaction, after the photon-proton interaction, we have a $K\bar{K}N$ three-body system which can decay to the $K\pi\Sigma$ channel due to Yukawa coupling of the K^- meson to a proton. In our approach, we decomposed the $\gamma p \to K^+(\pi\Sigma)$ reaction into two parts. The first part is the $\gamma p \to K\bar{K}N$ reaction and the second part is the $K\bar{K}N \to K^+(\pi\Sigma)$ reaction. In our calculations, we considered just the second part of the reaction. Thus, the processes in the dashed ellipse are included in the present work.

In this paper, the $\gamma p \to K^+(\pi\Sigma)^0$ reaction was studied by applying our approach based on the Alt-Grassberger-Sandhas (AGS) equations for the $K\bar{K}N$ three-body system [39]. To study the dependence of the results on two-body interactions, we used different types of phenomenological and chiral models of $\bar{K}N$ and $\bar{K}K$ interactions.

The paper is organized as follows: In Sec. II, a brief description of the Faddeev equations for a $K\bar{K}N$ three-body system is given. The formula for calculating the $\pi\Sigma$ mass spectrum and the two-body interactions, which are the inputs for the Faddeev equations are given in Sec. III. The discussion of the results can also be found in Sec. III. Finally, our conclusions are summarized in Sec. IV.

II. FADDEEV TREATMENT OF $K\bar{K}N$ THREE-BODY SYSTEM

The three-body calculations of the $K\bar{K}N$ system is based on the AGS form of the Faddeev equations [39]. We use separable potentials to describe the two-body interactions with

*Corresponding author: mnnasrabadi@ast.ui.ac.ir

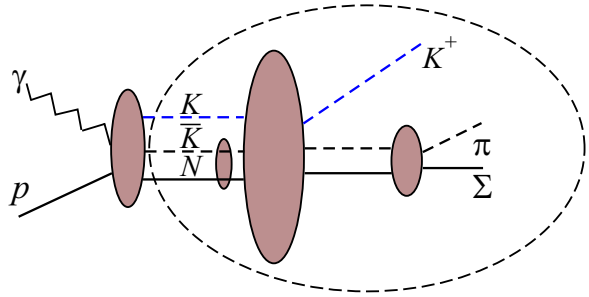

FIG. 1. Schematic depiction of the $\gamma p \to (\pi\Sigma)^0 + K^+$ reaction.

the form

$$V_I^{\alpha\beta}(k^\alpha, k^\beta; z) = g_I^\alpha(k^\alpha)\lambda_I^{\alpha\beta}(z)g_I^\beta(k^\beta), \tag{1}$$

where $g_I^\alpha(k^\alpha)$ is the form factor of the interacting two-body subsystem with relative momentum k^α and isospin I. The strength parameters of the interaction are shown by $\lambda_I^{\alpha\beta}$ and z is a two-body energy. To include the low-lying channels in the $\bar{K}N$-$\pi\Sigma$ and $\bar{K}K$-$\pi\pi$-$\pi\eta$ interactions, the potentials are labeled by α and β indexes. The separable form of the two-body T matrices are given by

$$T_I^{\alpha,\beta}(k^\alpha, k^\beta; z) = g_I^\alpha(k^\alpha)\tau_I^{\alpha,\beta}(z)g_I^\beta(k^\beta), \tag{2}$$

where the operator $\tau_I^{\alpha,\beta}(z)$ is the usual two-body propagator.

Using a separable potential for two-body interactions, the three-body Faddeev equations [18] in the AGS form can be given by

$$\begin{aligned}
&\mathcal{K}^{\alpha,\beta}_{i,j;I_i,I_j}(p_i, p_j; W) \\
&\quad = (1-\delta_{ij})\mathcal{M}^\alpha_{i,j;I_i,I_j}\left(p_i^\alpha, p_j^\alpha; W\right) \\
&\qquad + \sum_\gamma^4 \sum_{k,I_k} \int d^3p_k \mathcal{M}^\alpha_{i,k;I_i,I_k}\left(p_i^\alpha, p_k^\alpha; W\right)\tau^{\alpha,\gamma}_{k;I_k} \\
&\qquad \times \left(W - \frac{\left(p_k^\alpha\right)^2}{2\nu_k^\alpha}\right)\mathcal{K}^{\gamma,\beta}_{k,j;I_k,I_j}\left(p_k^\gamma, p_j^\beta; W\right).
\end{aligned} \tag{3}$$

Here, the operators $\mathcal{K}^{\alpha,\beta}_{i,j;I_i,I_j}$ are three-body transition amplitudes which describe the elastic and re-arrangement processes $[i+(jk)_{I_i}]^\alpha \to [j+(ki)_{I_j}]^\beta$ [18,40–42] and the operators $\mathcal{M}^\alpha_{i,j;I_i,I_j}$ are Born terms which describe the effective potential realized by exchanged particles. In this equation, W is the three-body energy and $W - \frac{(p_k^\alpha)^2}{2\nu_k^\alpha}$ is the energy of the interacting pair (ij), where $\nu_k^\alpha = m_k^\alpha(m_i^\alpha + m_j^\alpha)/(m_i^\alpha + m_j^\alpha + m_k^\alpha)$, is the reduced mass, when particle k is a spectator. Faddeev partition indexes $i, j, k = 1, 2, 3$ denote simultaneously an interacting pair and a spectator particle. The operators in the Faddeev Eq. (3) are also labeled by particle indexes α, β, and $\gamma = 1, 2, 3, 4$ to include the low-lying channels:

$$\begin{aligned}
&[\alpha = 1] : K\bar{K}N, [\alpha = 2] : K\pi\Sigma, \\
&[\alpha = 3] : \pi\pi N, [\alpha = 4] : \pi\eta N.
\end{aligned} \tag{4}$$

III. RESULTS AND DISCUSSION

Before we proceed to represent the discussion of the results, the two-body interactions should be defined. The two-body potentials are the basic ingredient of our three-body calculations for the $K\bar{K}N$ system. Defining the subsystems of the three-body $K\bar{K}N$ system, the main two-body interactions are $\bar{K}N$, $K\bar{K}$, and KN. The $\bar{K}N$ subsystem is coupled with $\pi\Sigma$ and $K\bar{K}$ is coupled with $\pi\pi$ and $\pi\eta$ in the $I = 0$ and $I = 1$ channels, respectively. Therefore, in the full Faddeev calculation of $K\bar{K}N$, one should also include the $K\pi\Sigma$, $\pi\pi N$, and $\pi\eta N$ channels. In the present work, first the one-channel AGS calculation was performed and the effect of the low-lying channels was taken into account effectively. Therefore, the two-body interactions in the low-lying channels were neglected and decaying to $\pi\Sigma$, $\pi\pi$, and $\pi\eta$ was included by using the so-called exact optical potentials [17]. In the present calculations, all potentials are in separable form having the form of Eq. (1).

To describe the coupled-channel $\bar{K}N$-$\pi\Sigma$ system, different models of interaction were used. We used four different phenomenological potentials plus one chiral potential for the $\bar{K}N$ interaction. The phenomenological potentials are energy independent and have the one- and two-pole structures of the $\Lambda(1405)$ resonance. Therefore, in Eq. (1), the strength parameters are energy independent. The parameters of the phenomenological potentials are given in Refs. [17,18]. In Ref. [17], the potentials are adjusted to reproduce the results of the KEK experiment and in Ref. [18] the potentials are adjusted to reproduce the results of the SIDDHARTA experiment. From now on, we refer to these phenomenological potentials as "KEK^X" and "SIDD^X," respectively ($X = 1, 2$). For example, SIDD^1 and SIDD^2 stand for the one- and two-pole versions of the SIDD potential, respectively. The chiral potential is energy dependent and reproduces the two-pole structure of the $\Lambda(1405)$ resonance. The parameters of the chiral-based potential are given in Ref. [43]. We refer to this potential as "Chiral." In Table I, the pole position of four different phenomenological (SIDD and KEK) potentials and one chiral-based $\bar{K}N$-$\pi\Sigma$ interaction are presented.

For the KN interaction with isospin $I = 0, 1$, we used a one-channel real potential. The range parameters of the potentials were set to 3.9 fm^{-1} and the strength parameters are adjusted to reproduce the KN scattering length. The experimental value of the scattering lengths for the $I = 0$ and $I = 1$ channels were set to $a_{KN}^{I=0} = -0.035$ fm and $a_{KN}^{I=1} = -0.310 \pm 0.003$ fm, respectively [44–46].

The $K\bar{K}$ interaction is attractive and, together with its coupled channels, dynamically generates the $f_0(980)$ and $a_0(980)$ resonances in the $I = 0$ and $I = 1$ channels, respectively. We constructed our own potentials for the coupled-channel $K\bar{K}$-$\pi\pi$ and $K\bar{K}$-$\pi\eta$ interactions in the form of Eq. (1) with form factors

$$g_\alpha^I(k_\alpha) = \frac{1}{k_\alpha^2 + \left(\Lambda_\alpha^I\right)^2}. \tag{5}$$

To define the parameters $\lambda^I_{\alpha\beta}$ and Λ^I_α, we used the mass and width of the f_0 and a_0 resonances, assuming that those are a quasibound state in the $K\bar{K}$ system and a resonance in

TABLE I. The model dependence of the $\bar{K}N$ pole position(s) (in MeV). The pole position of four different phenomenological interactions plus one chiral-based $\bar{K}N$-$\pi\Sigma$ interaction are represented. In the first row, X^1 and X^2 (X = SIDD, KEK) standing for the one- and two-pole versions of the SIDD and KEK potentials, respectively.

	SIDD^1	SIDD^2	KEK^1	KEK^2	Chiral
First pole	$1428.1 - i46.6$	$1418.1 - i56.9$	$1411.3 - i35.8$	$1410.8 - i35.9$	$1420.6 - i20.3$
Second pole		$1382.0 - i104.2$		$1380.8 - i104.8$	$1343.0 - i72.5$

the $\pi\pi$ and $\pi\eta$ channels, respectively. For the pole-energy of the f_0 and a_0 resonances, the mass of 980 MeV and the width of 80 MeV were used. Therefore, the $f_0(980)$ [$a_0(980)$] pole is located on first Riemann sheet of the $K\bar{K}$ channel and on the second Riemann sheet of the $\pi\pi$ ($\pi\eta$) channel. We also used the $K\bar{K}$ scattering length. For $K\bar{K}$ scattering length, we used the values reported in Ref. [47] ($a^{I=0}_{K\bar{K}} = -0.14 - i1.99$ fm and $a^{I=1}_{K\bar{K}} = 0.18 - i0.61$ fm).

A. The one-channel Alt-Grassberger-Sandhas calculations of the $K\bar{K}N$-$K\pi\Sigma$-$\pi\pi N$-$\pi\eta N$ system

In the present section, the low-lying channels of the $K\bar{K}N$ system has not been included directly and the one-channel Faddeev AGS equations were solved for three-body $K\bar{K}N$ system and we approximated the full coupled-channel interaction by using the so-called exact optical $\bar{K}N(-\pi\Sigma)$ and $\bar{K}N(-\pi\pi\text{-}\pi\eta)$ potentials [17]. Therefore, decay to the $K\pi\Sigma$, $\pi\pi N$, and $\pi\eta N$ channels is taken into account through the imaginary part of the optical $\bar{K}N(-\pi\Sigma)$ and $\bar{K}N(-\pi\pi\text{-}\pi\eta)$ potentials.

Since, the $K + (\bar{K}N)_{I=0}$ partition is the dominant state of the $K\bar{K}N$ three-body system, here, we supposed the $K + (\bar{K}N)_{I=0}$ partition as the initial state of the $K\bar{K}N$ system. Therefore, the Faddeev equations for the $K + (\bar{K}N)_{I=0}$ reaction will have the form

$$\begin{aligned}
\mathcal{K}^{1,1}_{K,K;I_K,0} &= +\mathcal{M}^{1}_{K,N;I_K,I_N}\tau^{11}_{N;I_N}\mathcal{K}^{1,1}_{N,K;I_N,0} + \mathcal{M}^{1}_{K,\bar{K};I_K,I_{\bar{K}}}\tau^{11}_{\bar{K};I_{\bar{K}}}\mathcal{K}^{1,1}_{\bar{K},K;I_{\bar{K}},0},\\
\mathcal{K}^{1,1}_{N,K;I_N,0} &= \mathcal{M}^{1}_{N,K;I_N,0} + \mathcal{M}^{1}_{N,K;I_N,I_K}\tau^{11}_{K;I_K}\mathcal{K}^{1,1}_{K,K;I_K,0} + \mathcal{M}^{1}_{N,\bar{K};I_N,I_{\bar{K}}}\tau^{11}_{\bar{K};I_{\bar{K}}}\mathcal{K}^{1,1}_{\bar{K},K;I_{\bar{K}},0},\\
\mathcal{K}^{1,1}_{\bar{K},K;I_{\bar{K}},0} &= \mathcal{M}^{1}_{\bar{K},K;I_{\bar{K}},0} + \mathcal{M}^{1}_{\bar{K},K;I_{\bar{K}},I_K}\tau^{11}_{K;I_K}\mathcal{K}^{1,1}_{K,K;I_K,0} + \mathcal{M}^{1}_{\bar{K},N;I_{\bar{K}},I_N}\tau^{11}_{N;I_N}\mathcal{K}^{1,1}_{N,K;I_N,0}.
\end{aligned} \tag{6}$$

To study the possible signature of the Λ(1405) resonance in the $\pi\Sigma$ mass spectra in the $K + (\bar{K}N)_{I=0} \to K\pi\Sigma$ reaction, first one should define the scattering amplitude. Given that we do not include the low-lying channels directly into the calculations, the only Faddeev amplitude which contributes in the scattering amplitude is $\mathcal{K}^{1,1}_{K,K;I_K,0}(p_K, P_K; W)$ ($I_K = 0, 1$). Therefore, the scattering amplitude can be expressed as

$$\begin{aligned}
&T_{(\pi\Sigma)+K\leftarrow(\bar{K}N)_{I=0}+K}(\vec{k}_K, \vec{p}_K, \vec{P}_K; W)\\
&\quad= \sum_{I_K} g^{I_K}_2(\vec{k}_K)\tau^{21}_{K;I_K}\left(W - \frac{p_K^2}{2\nu_K}\right)\mathcal{K}^{1,1}_{K,K;I_K,0}(p_K, P_K; W),
\end{aligned} \tag{7}$$

where $\vec{k}_i$ is the relative momentum between the interacting pair (jk) and $\vec{P}_K$ is the initial momentum of the spectator K in the $K\bar{K}N$ center of mass. The quantity $\mathcal{K}^{1,1}_{i,j;I_i,I_j}$ is the Faddeev amplitude, driven from Eq. (6).

Using Eq. (7), we define the cross section of $K + (\bar{K}N)_{I=0} \to K + (\pi\Sigma)^0$ scattering as follows:

$$\begin{aligned}
\frac{d\sigma}{dE_K} &= \frac{\omega_{(\bar{K}N)}\omega_K}{WP_K}\frac{m_\pi m_\Sigma m_K}{m_\pi + m_\Sigma + m_K}\int d\Omega_{p_K} d\Omega_{k_K} p_K k_K\\
&\quad\times \sum_{if} |T_{(\pi\Sigma)^0+K\leftarrow(\bar{K}N)_{I=0}+K}(\vec{k}_K, \vec{p}_K, \vec{P}_K; W)|^2,
\end{aligned} \tag{8}$$

where E_K is the kaon energy in the center-of-mass frame and is defined by

$$E_K = m_K + \frac{p_K^2}{2\nu'_K}, \quad \nu'_K = \frac{m_K(m_\pi + m_\Sigma)}{m_K + m_\pi + m_\Sigma}, \tag{9}$$

and the energies $\omega_{(\bar{K}N)}$ and ω_K are the kinetic energies of K and $\bar{K}N$ in the initial state.

Using Eq. (8), we calculated the $\pi\Sigma$ mass spectra for the $K + (\bar{K}N)_{I=0}$ reaction. The calculated $\pi\Sigma$ mass spectrum for different $\bar{K}N$ models of interaction are depicted in Fig. 2. In addition to the calculated mass spectra, the extracted data of CLAS experiment are also presented. The CLAS data are accessible for several energy bins, but in the present work, we calculated the $\pi\Sigma$ mass spectrum for two values of energy. In the upper row, the total energy of the three-body system in the center-of-mass frame is $W = 2$ GeV, and in the lower row the total energy of the system is $W = 2.5$ GeV. We used one-pole and two-pole versions of the KEK and SIDD potentials and also the chiral-based interaction to describe the $\bar{K}N$ interaction. The $\pi\Sigma$ mass spectra are calculated for all combinations of charges, i.e., $\pi^+\Sigma^-$, $\pi^-\Sigma^+$, and $\pi^0\Sigma^0$.

Since the input energy of the AGS equations is real, the moving singularities which are caused by the open channels will appear in the three-body amplitudes. To remove the moon-shaped singularities, we followed the same procedure implemented in Refs. [48,49].

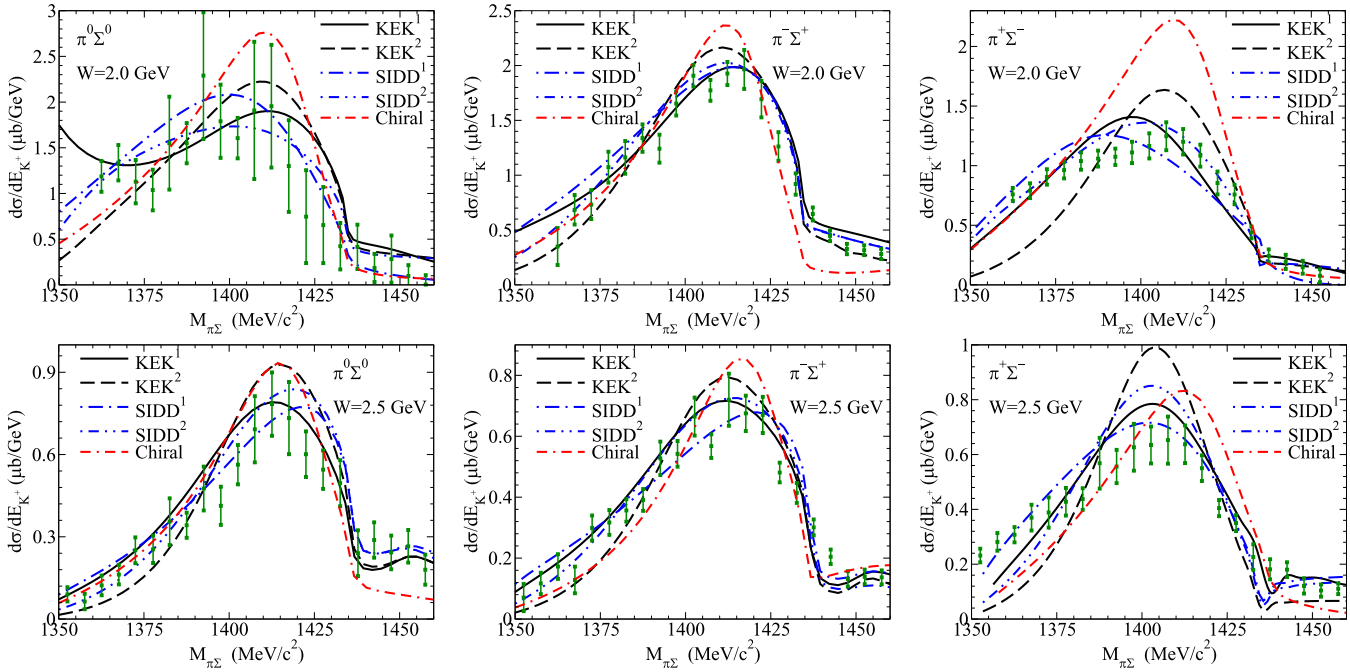

FIG. 2. Comparison of the obtained results for $\pi\Sigma$ mass spectra in the $K + (\bar{K}N)_{I=0}$ reaction with the extracted experimental results [20,21] corresponding to the $\gamma p \to (\pi\Sigma)^0 + K^+$ reaction. Different types of $\bar{K}N$-$\pi\Sigma$ potentials were used. We used the one- and two-pole versions of the SIDD and KEK potentials [17,18] and also a chiral potential [43]. The initial energy of the system is around $E = 2.0$ (upper row) and $E = 2.5$ GeV (lower row). The black solid and black dashed lines show the mass spectra with one- and two-pole models of the KEK potential, respectively. The results for one- and two-pole models of the SIDD potential are depicted by the blue dash-dotted and blue dash-dot-dotted curves. Finally, the chiral results are represented by red dash-dash-dotted line.

Comparing the experimental and theoretical results presented in Fig. 2, we calculated χ^2 for each model of $\bar{K}N$ interaction:

$$\chi^2 = \sum_{i=1}^{N} \frac{\left(N_i - \frac{d\sigma}{dE_K}\right)^2}{(\sigma_i)^2}, \tag{10}$$

where N denotes the number of data points included in the present fitting process. Here, $\frac{d\sigma}{dE_K}$ and N_i denote the theoretical and experimental values for $K + (\bar{K}N)_{I=0}$ differential cross sections at energy W. The calculated values for χ^2 are given in Table II [the columns with the symbol (A) present the results of one-channel AGS calculations]. In our calculations, we used 18 points of experimental results, starting from $M_{\pi\Sigma} =$ 1352 to 1437 MeV/c^2.

In addition to the $\bar{K}N$ interaction, the $K\bar{K}$ interaction is important in studying the dynamics of the $K\bar{K}N$ and may affect the experimental observable related to this system. To study the dependence of the mass spectra on the $K\bar{K}$ model of interaction, we also constructed several energy-independent potentials by varying the mass and width of the $f_0(980)$ and $a_0(980)$ resonances. Figure 3 shows the variation of the $\pi^0\Sigma^0$ mass spectrum with respect to the real (left panel) and imaginary (right panel) part of the $\bar{K}K$ pole position at energy $W = 2.5$ GeV. In the left panel, the width of the $f_0(980)$ and $a_0(980)$ resonances is fixed to 80 MeV and their mass

TABLE II. The dependence of the χ^2 parameter on the $\bar{K}N$ model of interaction in different particle channels. The results obtained in Secs. III A–III C are labeled by (A), (B), and (C), respectively.

	KEK^1			KEK^2			SIDD^1			SIDD^2			Chiral		
$W = 2.0$ GeV	(A)	(B)	(C)	(A)	(B)	(C)	(A)	(B)	(C)	(A)	(B)	(C)	(A)	(B)	(C)
$\chi^2(\pi^0\Sigma^0)$	30.5	14.4	17.5	68.1	28.9	26.2	62.8	11.2	10.6	23.8	16.3	11.3	52.2	24.8	28.8
$\chi^2(\pi^-\Sigma^+)$	42.5	32.7	26.8	79.0	79.8	48.2	27.9	14.4	18.9	26.3	21.5	22.3	316	97.7	37.7
$\chi^2(\pi^+\Sigma^-)$	82.7	99.8	85.0	343	362	227	95.0	42.5	26.0	31.2	92.6	81.2	313	312	232
$W = 2.5$ GeV	(A)	(B)	(C)	(A)	(B)	(C)	(A)	(B)	(C)	(A)	(B)	(C)	(A)	(B)	(C)
$\chi^2(\pi^0\Sigma^0)$	27.7	17.4	11.2	62.6	49.7	24.4	20.9	13.9	13.2	30.9	31.2	23.3	79.5	12.2	12.5
$\chi^2(\pi^-\Sigma^+)$	80.6	91.5	39.0	168	83.4	46.0	82.3	37.7	16.9	106	31.5	32.5	208	22.5	43.1
$\chi^2(\pi^+\Sigma^-)$	100.7	137	66.8	448	478	299	58.7	198	39.7	217	330	144	270	102	67.5

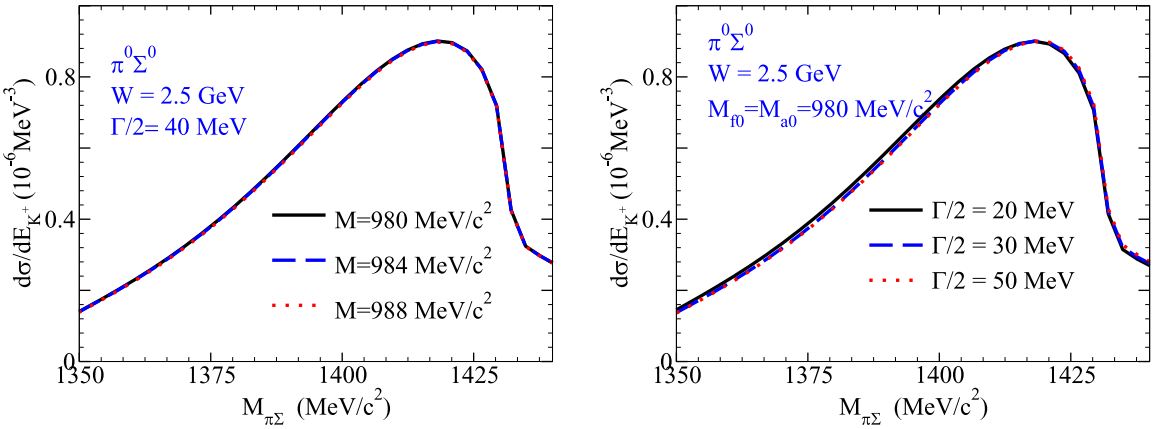

FIG. 3. The dependence of the $\pi^0\Sigma^0$ mass spectra on the real (upper panel) and imaginary part (lower panel) of the $\bar{K}K$ pole position.

varied from 980 to 988 MeV/c^2. In the right panel the mass of the resonances is fixed at 980 MeV/c^2 and the width was changed. As one can see from Fig. 3, the $f_0(980)$ and $a_0(980)$ pole position variation cannot change the $\pi^0\Sigma^0$ mass spectrum, effectively.

B. The full coupled-channel Alt-Grassberger-Sandhas calculations of the $K\bar{K}N$-$K\pi\Sigma$-$\pi\pi N$-$\pi\eta N$ system

In Sec. III A, we solved the one-channel AGS equations for the $K\bar{K}N$ system, and decaying to the low-lying channels is included by using the so-called exact optical potential for the $\bar{K}N$ and $\bar{K}K$ interactions. In the one-channel Faddeev calculations, the effect of the $\tau_{\pi\Sigma\to\pi\Sigma}$ amplitude was excluded. Based on the chiral unitary approach, the first and second pole of Λ(1405) have clearly a different coupling nature with respect to the meson-baryon channels; the higher-energy pole dominantly couples to the $\bar{K}N$ channel, while the lower-energy pole strongly couples to the $\pi\Sigma$ channel. Due to the different coupling nature of these resonances, the shape of the Λ(1405) spectrum can be different depending on the initial and final channels. In the $\bar{K}N\to\pi\Sigma$ amplitude, the initial $\bar{K}N$ channel gets a greater contribution from the higher pole with a larger weight. Consequently, the spectrum shape has a peak around 1420 MeV coming from the higher pole [50,51]. This is obviously different from the $\pi\Sigma\to\pi\Sigma$ spectrum which is largely affected by the lower pole. Therefore, the extracted mass spectra in Sec. III A cannot reproduce exactly what we would see in an experiment.

In addition to the above-mentioned reaction, we need an interaction model for ΣK, πK, πN, and ηN subsystems. To describe the ΣK interaction with isospin $I = 1/2$, $3/2$, we used a one-term complex potential for the $I = 1/2$ channel and a real potential for the $I = 3/2$ channel. To define the parameters of the ΣK interaction, we used the ΣK scattering length and the pole energy of the $N^*(1535)$ resonance ($z_{pole} = 1543 - i46$ MeV) [52]. To describe the πN interaction, we used the potential given in Ref. [43]. To define the πK interaction in the $I = 1/2$ channel, we used a complex potential reproducing the pole energy of the $K^*(892)$ resonance ($z_{pole} = 770 - i250$ MeV) [53] and the parameters of the real πK potential with isospin $I = 3/2$ were adjusted to reproduce the πK phase shifts [53].

To calculate the $\pi\Sigma$ mass spectrum for the $K + (\bar{K}N)_{I=0}$ reaction, we solved the Faddeev equations for the coupled-channel $K\bar{K}N$-$K\pi\Sigma$-$\pi\pi$-$\pi\eta$ system which have the form

$$
\begin{aligned}
\mathcal{K}^{1,1}_{K,K;I_K,0} &= \mathcal{M}^{1}_{K,\bar{K};I_K,I_{\bar{K}}}\tau^{11}_{\bar{K};I_{\bar{K}}}\mathcal{K}^{1,1}_{\bar{K},K;I_{\bar{K}},0} + \mathcal{M}^{1}_{K,N;I_K,I_N}\tau^{11}_{N;I_N}\mathcal{K}^{1,1}_{N,K;I_N,0} \\
&\quad + \mathcal{M}^{1}_{K,N;I_K,I_N}\tau^{13}_{N;I_N}\mathcal{K}^{3,1}_{N,K;I_N,0} + \mathcal{M}^{1}_{K,N;I_K,I_N}\tau^{14}_{N;I_N}\mathcal{K}^{4,1}_{N,K;I_N,0}, \\
\mathcal{K}^{1,1}_{\bar{K},K;I_{\bar{K}},0} &= \mathcal{M}^{1}_{\bar{K},K;I_{\bar{K}},0} + \mathcal{M}^{1}_{\bar{K},K;I_{\bar{K}},I_K}\tau^{11}_{K;I_K}\mathcal{K}^{1,1}_{K,K;I_K,0} + \mathcal{M}^{1}_{\bar{K},K;I_{\bar{K}},I_K}\tau^{12}_{K;I_K}\mathcal{K}^{2,1}_{K,K;I_K,0} \\
&\quad + \mathcal{M}^{1}_{\bar{K},N;I_{\bar{K}},I_N}\tau^{11}_{N;I_N}\mathcal{K}^{1,1}_{N,K;I_N,0} + \mathcal{M}^{1}_{\bar{K},N;I_{\bar{K}},I_N}\tau^{14}_{N;I_N}\mathcal{K}^{4,1}_{N,K;I_N,0}, \\
\mathcal{K}^{1,1}_{N,K;I_N,0} &= \mathcal{M}^{1}_{N,K;I_N,0} + \mathcal{M}^{1}_{N,K;I_N,I_K}\tau^{11}_{K;I_K}\mathcal{K}^{1,1}_{K,K;I_K,0} + \mathcal{M}^{1}_{N,\bar{K};I_N,I_{\bar{K}}}\tau^{11}_{\bar{K};I_{\bar{K}}}\mathcal{K}^{1,1}_{\bar{K},K;I_{\bar{K}},0} + \mathcal{M}^{1}_{N,K;I_N,I_K}\tau^{11}_{K;I_K}\mathcal{K}^{1,1}_{K,K;I_K,0}, \\
\mathcal{K}^{2,1}_{K,K;I_N,0} &= \mathcal{M}^{2}_{K,\pi;I_K,I_\pi}\tau^{22}_{\pi;I_\pi}\mathcal{K}^{2,1}_{\pi,K;I_\pi,0} + \mathcal{M}^{2}_{K,\Sigma;I_K,I_\Sigma}\tau^{22}_{\Sigma;I_\Sigma}\mathcal{K}^{2,1}_{\Sigma,K;I_\Sigma,0}, \\
\mathcal{K}^{2,1}_{\pi,K;I_N,0} &= \mathcal{M}^{2}_{\pi,K;I_K,I_K}\tau^{22}_{K;I_K}\mathcal{K}^{2,1}_{K,K;I_K,0} + \mathcal{M}^{2}_{\pi,\Sigma;I_K,I_\Sigma}\tau^{22}_{\Sigma;I_\Sigma}\mathcal{K}^{2,1}_{\Sigma,K;I_\Sigma,0} + \mathcal{M}^{2}_{\pi,K;I_K,I_K}\tau^{21}_{K;I_K}\mathcal{K}^{1,1}_{K,K;I_K,0}, \\
\mathcal{K}^{2,1}_{\Sigma,K;I_N,0} &= \mathcal{M}^{2}_{\Sigma,K;I_K,I_K}\tau^{22}_{K;I_K}\mathcal{K}^{2,1}_{K,K;I_K,0} + \mathcal{M}^{2}_{\Sigma,\pi;I_K,I_K}\tau^{22}_{K;I_\pi}\mathcal{K}^{2,1}_{\pi,K;I_\pi,0} + \mathcal{M}^{2}_{\Sigma,K;I_K,I_K}\tau^{21}_{K;I_K}\mathcal{K}^{1,1}_{K,K;I_K,0}, \\
\bar{\mathcal{K}}^{3,1}_{\pi,K;I_\pi,0} &= \mathcal{M}^{3}_{\pi_1,\pi_2;I_{\pi_1},I_{\pi_2}}\tau^{33}_{\pi_2;I_{\pi_2}}\bar{\mathcal{K}}^{3,1}_{\pi,K;I_\pi,0} + 2\mathcal{M}^{3}_{\pi_1,N;I_{\pi_2},I_N}\tau^{33}_{N;I_N}\bar{\mathcal{K}}^{3,1}_{N,K;I_N,0} + 2\mathcal{M}^{3}_{\pi_1,N;I_{\pi_2},I_N}\tau^{31}_{N;I_N}\bar{\mathcal{K}}^{1,1}_{N,K;I_N,0}, \\
\mathcal{K}^{3,1}_{N,K;I_N,0} &= \mathcal{M}^{3}_{N,\pi_1;I_N,I_{\pi_1}}\tau^{33}_{\pi_1;I_{\pi_1}}\bar{\mathcal{K}}^{3,1}_{\pi,K;I_\pi,0},
\end{aligned}
$$

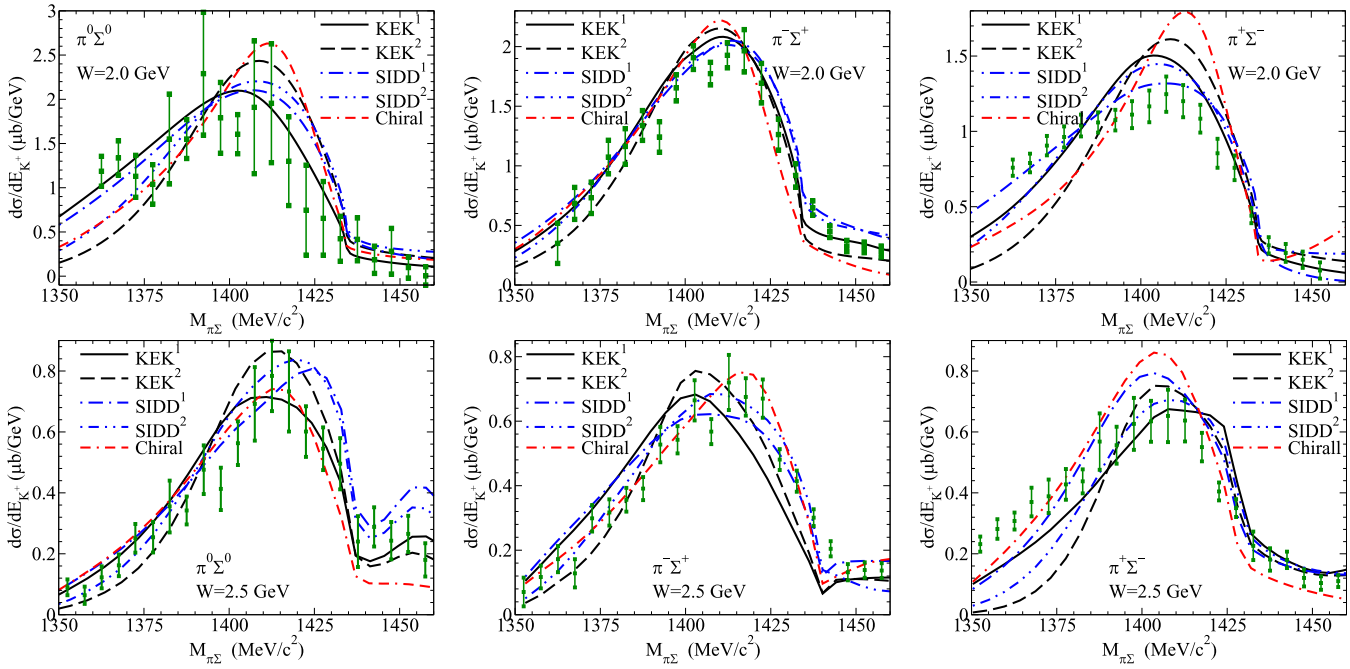

FIG. 4. The $\pi\Sigma$ mass spectra for the $\gamma p \to (\pi\Sigma)^0 + K^+$ reaction. The descriptions are the same as in Fig. 2, but in the present calculations, the full coupled-channel Faddeev AGS equations for the $K\bar{K}N$-$K\pi\Sigma$-$\pi\pi N$-$\pi\eta N$ system are solved.

$$\mathcal{K}^{4,1}_{\pi,K;I_\pi,0} = \mathcal{M}^{4}_{\pi,\eta;I_\pi,I_\eta}\tau^{44}_{\eta;I_\eta}\mathcal{K}^{4,1}_{\eta,K;I_\eta,0} + \mathcal{M}^{4}_{\pi,N;I_\pi,I_N}\tau^{44}_{N;I_N}\mathcal{K}^{4,1}_{N,K;I_N,0} + \mathcal{M}^{4}_{\pi,N;I_\pi,I_N}\tau^{41}_{N;I_N}\mathcal{K}^{1,1}_{N,K;I_N,0},$$
$$\mathcal{K}^{4,1}_{\eta,K;I_\eta,0} = \mathcal{M}^{4}_{\eta,\pi;I_\eta,I_\pi}\tau^{44}_{\pi;I_\pi}\mathcal{K}^{4,1}_{\pi,K;I_\pi,0} + \mathcal{M}^{4}_{\eta,N;I_\eta,I_N}\tau^{44}_{N;I_N}\mathcal{K}^{4,1}_{N,K;I_N,0} + \mathcal{M}^{4}_{\eta,N;I_\eta,I_N}\tau^{41}_{N;I_N}\mathcal{K}^{1,1}_{N,K;I_N,0},$$
$$\mathcal{K}^{4,1}_{N,K;I_N,0} = \mathcal{M}^{4}_{N,\pi;I_N,I_\pi}\tau^{44}_{\pi;I_\pi}\mathcal{K}^{4,1}_{\pi,K;I_\pi,0} + \mathcal{M}^{4}_{N,\eta;I_N,I_\eta}\tau^{44}_{\eta;I_\eta}\mathcal{K}^{4,1}_{\eta,K;I_\eta,0}. \quad (11)$$

Since there are two identical pions in the $\pi\pi N$ channel, the operators in this channel should be symmetrized. Therefore, the operators $\mathcal{K}^{3,1}_{\pi_1,K;I_{\pi_1},0}$ and $\mathcal{K}^{3,1}_{\pi_2,K;I_{\pi_2},0}$ are replaced by $\bar{\mathcal{K}}^{3,1}_{\pi,K;I_\pi,0}$, which is given by

$$\bar{\mathcal{K}}^{3,1}_{\pi,K;I_\pi,0} = \mathcal{K}^{3,1}_{\pi_1,K;I_{\pi_1},0} + \mathcal{K}^{3,1}_{\pi_2,K;I_{\pi_2},0}. \quad (12)$$

The scattering amplitude for the $K + (\bar{K}N)_{I=0} \to K + (\pi\Sigma)$ reaction in terms of the Faddeev transition amplitudes can be given by

$$\begin{aligned}
&T_{(\pi\Sigma)K\leftarrow(\bar{K}N)_{I=0}+K}(\vec{k}_K,\vec{p}_K,P_K;W)\\
&= \sum_{I_K} g^2_{K;I_K}(\vec{k}_K)\tau^{21}_{K;I_K}(W-E_K(\vec{p}_K))\mathcal{K}^{1,1}_{K,K;I_K,0}(p_K,P_K;W)\\
&\quad + \sum_{I_K} g^2_{K;I_K}(\vec{k}_K)\tau^{22}_{K;I_K}(W-E_K(\vec{p}_K))\mathcal{K}^{2,1}_{K,K;I_K,0}(p_K,P_K;W)\\
&\quad + \sum_{I_\pi}\sum_{I_K}\langle[\pi\otimes\Sigma]_{I_K}\otimes K \mid \pi\otimes[\Sigma\otimes K]_{I_\pi}\rangle g^2_{\pi;I_\pi}(\vec{k}_\pi)\\
&\quad \times\tau^{22}_{\pi;I_\pi}(W-E_\pi(\vec{p}_\pi))\mathcal{K}^{21}_{\pi,K;I_\pi,0}(p_\pi,P_K;W)\\
&\quad + \sum_{I_\Sigma}\sum_{I_K}\langle[\pi\otimes\Sigma]_{I_K}\otimes K \mid \Sigma\otimes[\pi\otimes K]_{I_\Sigma}\rangle g^2_{\Sigma;I_\Sigma}(\vec{k}_\Sigma)\\
&\quad \times\tau^{22}_{\Sigma;I_\Sigma}(W-E_\Sigma(\vec{p}_\Sigma))\mathcal{K}^{21}_{\Sigma,K;I_\Sigma,0}(p_\Sigma,P_K;W). \quad (13)
\end{aligned}$$

As one can see from Eq. (13), in coupled-channel calculations plus the $\mathcal{K}^{1,1}_{K,K;I_K,0}$ amplitude, the effect of the $\mathcal{K}^{2,1}_{K,K;I_K,0}$, $\mathcal{K}^{21}_{\pi,K;I_\pi,0}$, and $\mathcal{K}^{21}_{\Sigma,K;I_\Sigma,0}$ amplitude are also included, which accordingly produces a more precise mass spectrum for $\pi\Sigma$. Inserting the new scattering amplitude [Eq. (13)] in Eq. (8), one can calculate the $\pi\Sigma$ mass spectrum for the $K + (\bar{K}N)_{I=0} \to K + (\pi\Sigma)^0$ reaction. In Fig. 4, we calculated the $\pi\Sigma$ mass spectrum using different potential models for the $\bar{K}N$-$\pi\Sigma$ interaction. We also calculated the χ^2 values for each model of interaction, which are presented in Table II [the columns shown by (B)]. By comparing the results using one-channel and coupled-channel Faddeev equations, it may be possible to study the effect of the $\tau_{\pi\Sigma\to\pi\Sigma}$ amplitude on the $\pi\Sigma$ invariant mass. As can be seen in Table. II, the inclusion of he $\tau_{\pi\Sigma\to\pi\Sigma}$ amplitude can reduce the χ^2 values, especially in the $\pi^0\Sigma^0$ channel.

C. Dependence of the $\pi\Sigma$ mass spectra on the initial channel

The extracted results in Refs. [46,54,55] suggest that the $K\bar{K}N$ state can be understood by the structure of simultaneous coexistence of $\Lambda(1405) + K$ and $a_0(980) + N$ clusters and the $\bar{K}$ meson is shared by both $\Lambda(1405)$ and $a_0(980)$ at the same time. In Figs. 2 and 4, it was supposed that the initial state of the $K\bar{K}N$ system is $(\bar{K}N)_{I=0} + K$ and the $\pi\Sigma$ mass spectrum was calculated for the $(\bar{K}N)_{I=0} +$

K reaction. Now, in the present subsection, we take into account all possible channels of the $K\bar{K}N$ system, namely, $(\bar{K}N)_{I=0,1}+K$, $(K\bar{K})^{J=0,1}_{I=0,1}+N$, and $(KN)_{I=0,1}+\bar{K}$. Therefore, the initial state is a mixture of the mentioned partitions. The Faddeev equations in Eq. (11) are related to the initial state $K+(\bar{K}N)_{I=0}$. Therefore, by changing the initial state, the Faddeev equations must be changed. The Faddeev equations in the $\alpha=1$ channel are given by

$$\begin{aligned}
\mathcal{K}^{1,1}_{K,x;I_K,I_xJ} &= (1-\delta_{Kx})\mathcal{M}^{1}_{K,x;I_K,I_xJ}\mathcal{M}^{1}_{K,\bar{K};I_K,I_{\bar{K}}}\tau^{11}_{\bar{K};I_{\bar{K}}}\mathcal{K}^{1,1}_{\bar{K},x;I_{\bar{K}},I_xJ}+\mathcal{M}^{1}_{K,N;I_K,I_N}\tau^{11}_{N;I_N}\mathcal{K}^{1,1}_{N,x;I_N,I_xJ}\\
&\quad+\mathcal{M}^{1}_{K,N;I_K,I_N}\tau^{13}_{N;I_N}\mathcal{K}^{3,1}_{N,x;I_N,I_xJ}+\mathcal{M}^{1}_{K,N;I_K,I_N}\tau^{14}_{N;I_N}\mathcal{K}^{4,1}_{N,x;I_N,I_xJ},\\
\mathcal{K}^{1,1}_{\bar{K},x;I_{\bar{K}},I_xJ} &= (1-\delta_{\bar{K}x})\mathcal{M}^{1}_{\bar{K},x;I_{\bar{K}},I_xJ}+\mathcal{M}^{1}_{\bar{K},K;I_{\bar{K}},I_K}\tau^{11}_{K;I_K}\mathcal{K}^{1,1}_{K,x;I_K,I_xJ}+\mathcal{M}^{1}_{\bar{K},K;I_{\bar{K}},I_K}\tau^{12}_{K;I_K}\mathcal{K}^{2,1}_{K,x;I_K,I_xJ}\\
&\quad+\mathcal{M}^{1}_{\bar{K},N;I_{\bar{K}},I_N}\tau^{11}_{N;I_N}\mathcal{K}^{1,1}_{N,x;I_N,I_xJ}+\mathcal{M}^{1}_{\bar{K},N;I_{\bar{K}},I_N}\tau^{14}_{N;I_N}\mathcal{K}^{4,1}_{N,x;I_N,I_xJ},\\
\mathcal{K}^{1,1}_{N,x;I_N,I_xJ} &= (1-\delta_{Nx})\mathcal{M}^{1}_{N,x;I_N,I_xJ}+\mathcal{M}^{1}_{N,K;I_N,I_K}\tau^{11}_{K;I_K}\mathcal{K}^{1,1}_{K,x;I_K,I_xJ}+\mathcal{M}^{1}_{N,\bar{K};I_N,I_{\bar{K}}}\tau^{11}_{\bar{K};I_{\bar{K}}}\mathcal{K}^{1,1}_{\bar{K},x;I_{\bar{K}},I_xJ}\\
&\quad+\mathcal{M}^{1}_{N,K;I_N,I_K}\tau^{11}_{K;I_K}\mathcal{K}^{1,1}_{K,x;I_K,I_xJ}.
\end{aligned}\tag{14}$$

Depending on the initial state, the spectator particle x and the quantum numbers I_x and J (isospin and spin of the interacting pair) can be given by

$$\begin{aligned}
&x=K: K+(\bar{K}N)_{I_xJ}J=0; \quad I_x=0,1,\\
&x=\bar{K}: \bar{K}+(KN)_{I_xJ}J=0; \quad I_x=0,1,\\
&x=N: N+(K\bar{K})_{I_xJ}J=0,1; \quad I_x=0,1,
\end{aligned}\tag{15}$$

and, finally, in the $\alpha=2,3,4$ channels, just the indexes of the Faddeev amplitudes must be changed:

$$\mathcal{K}^{\alpha,1}_{i,K;I_K,0}\rightarrow\mathcal{K}^{\alpha,1}_{i,x;I_K,I_xJ}.\tag{16}$$

Using Eqs. (14)–(16), we define the scattering amplitude of the $K\bar{K}N\rightarrow K+(\pi\Sigma)^0$ reaction as follows:

$$\begin{aligned}
&T_{(\pi\Sigma)K\leftarrow(K\bar{K}N)}(\vec{k}_K,\vec{p}_K,P_x;W)\\
&=\sum_{x,I_x,J}\Bigg\{\sum_{I_K}g^2_{K;I_K}(\vec{k}_K)\tau^{21}_{K;I_K}[W-E_K(\vec{p}_K)]\\
&\quad\times\mathcal{K}^{1,1}_{K,x;I_K,I_xJ}(p_K,P_x;W)\\
&\quad+\sum_{I_K}g^2_{K;I_K}(\vec{k}_K)\tau^{22}_{K;I_K}[W-E_K(\vec{p}_K)]\\
&\quad\times\mathcal{K}^{2,1}_{K,x;I_K,I_xJ}(p_K,P_x;W)\\
&\quad+\sum_{I_\pi}\sum_{I_K}\langle[\pi\otimes\Sigma]_{I_K}\otimes K\mid\pi\otimes[\Sigma\otimes K]_{I_\pi}\rangle g^2_{\pi;I_\pi}(\vec{k}_\pi)\\
&\quad\times\tau^{22}_{\pi;I_\pi}[W-E_\pi(\vec{p}_\pi)]\mathcal{K}^{21}_{\pi,x;I_\pi,I_xJ}(p_\pi,P_x;W)\\
&\quad+\sum_{I_\Sigma}\sum_{I_K}\langle[\pi\otimes\Sigma]_{I_K}\otimes K\mid\Sigma\otimes[\pi\otimes K]_{I_\Sigma}\rangle g^2_{\Sigma;I_\Sigma}(\vec{k}_\Sigma)\\
&\quad\times\tau^{22}_{\Sigma;I_\Sigma}[W-E_\Sigma(\vec{p}_\Sigma)]\mathcal{K}^{21}_{\Sigma,x;I_\Sigma,I_xJ}(p_\Sigma,P_x;W)\Bigg\}.
\end{aligned}\tag{17}$$

In Fig. 5, the $\pi\Sigma$ mass spectrum was calculated for different potentials of the $\bar{K}N$-$\pi\Sigma$ interaction, including all initial channels of the $K\bar{K}N$ system. The extracted χ^2 values are also presented in Table II [the columns shown by (C)]. Comparing the results in the (C) columns for each model of interaction and scattering energy, one can see that the full coupled calculations including all initial channels can better reproduce the experimental results. Looking at Table II one can clearly see that, for the SIDD[1] potential, the values obtained for χ^2 are considerably smaller than those obtained by other potentials for all particle channels and kaon incident energies. Therefore, such a combined study at two different initial energies shows a big potential to discriminate between possible mechanisms of the formation of the Λ(1405) resonance.

D. Dependence of χ^2 on $\bar{K}N$ pole position

In Sec. III B, it was shown that the SIDD[1] potential with one-pole nature of the Λ(1405) resonance can reproduce the experimental results with smaller values of χ^2. In the present section, we study the dependence of the χ^2 parameter on the mass and width of the Λ(1405) resonance. Toward this goal, we constructed a coupled-channel $\bar{K}N$-$\pi\Sigma$ potential having a one-pole nature of Λ(1405) as a Feshbach resonance [56–58]. To define the parameters of the model, we used the following experimental data:

(1) Mass and width of the Λ(1405) resonances. Assuming that it is a quasibound state in the $\bar{K}N$ channel and a resonance in the $\pi\Sigma$ channel.

(2) The K^-p scattering length. For the K^-p scattering length, we used the values reported in Ref. [59]:

$$a_{K^-p}=-0.65+i0.81\ \text{fm}.\tag{18}$$

(3) The γ branching ratio, which is given by

$$\gamma=\frac{\Gamma(K^-p\rightarrow\pi^+\Sigma^-)}{\Gamma(K^-p\rightarrow\pi^-\Sigma^+)}=2.36\pm0.04.\tag{19}$$

(4) Elastic $K^-p\rightarrow K^-p$ total cross section.

We studied the dependence of the $\pi^0\Sigma^0$ mass spectrum on the $\bar{K}N$ pole position at $W=2.5$ GeV. In Fig. 6, the variation of the χ^2 values with respect to the real (left panel) and imaginary (right panel) part of the $\bar{K}N$ pole position for $\pi^0\Sigma^0$ mass spectra at energy $W=2.5$ GeV are depicted. In the left panel, the imaginary part of the $\bar{K}N$ pole position is

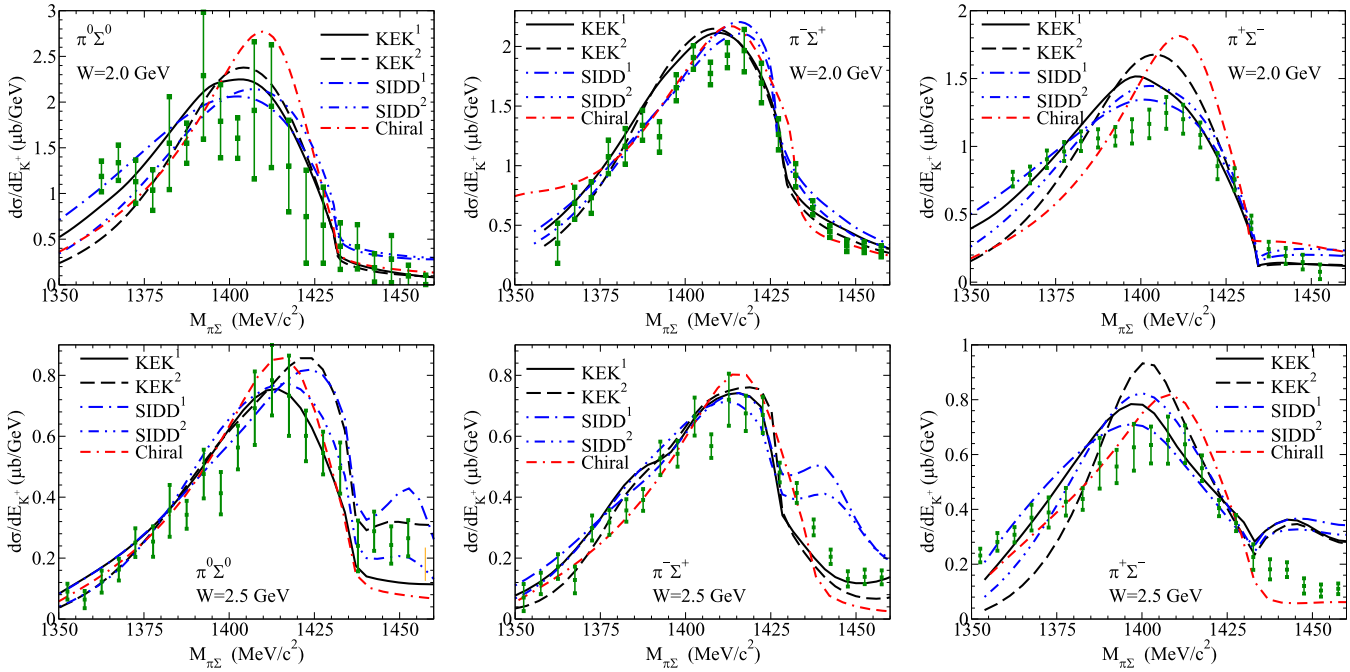

FIG. 5. The $\pi\Sigma$ mass spectra for the $\gamma p \to (\pi\Sigma)^0 + K^+$ reaction. The descriptions are same as in Fig. 2, but in the present calculations, the full coupled-channel Faddeev AGS equations for the $K\bar{K}N$-$K\pi\Sigma$-$\pi\pi N$-$\pi\eta N$ system are solved and all possible initial states of the $K\bar{K}N$ system are included.

fixed to be 28 MeV and in the right panel the real part of the pole position is 1417 MeV. As one can see, in the left panel, the mass of 1417 MeV/c^2 gives us the minimum value of the χ^2 parameter and in the right panel the width of 56 MeV was extracted for the $\Lambda(1405)$ resonance.

In the present calculations, the best fit was extracted just by taking into account the effect of the $\Lambda(1405)$ resonance, but there are other factors which may also have important effects on the results obtained here. The first one is the $\Sigma(1385)$ resonance; to be more precise, one should include also the effect of $\Sigma(1385)$ resonance which may change the extracted results. In particular, to find a better fit in the energy region below 1400 MeV, the inclusion of the $\Sigma(1385)$ resonance could be important. One can extend these calculations to include the effect of the $\Sigma(1385)$ resonance.

The two-body interactions are driven nonrelativistically. Therefore, in the present calculations, the nonrelativistic Faddeev equations were solved for the $K\bar{K}N$ system. One can also include the relativistic corrections by employing the methods presented in Refs. [60,61]. The kinetic energy of the system under consideration in this calculation is between 100 and 600 MeV in the $K\bar{K}N$ channel and is higher in low-lying channels. Comparing this kinetic energy with the average mass of the pion of 139 MeV/c^2, one can conclude that the

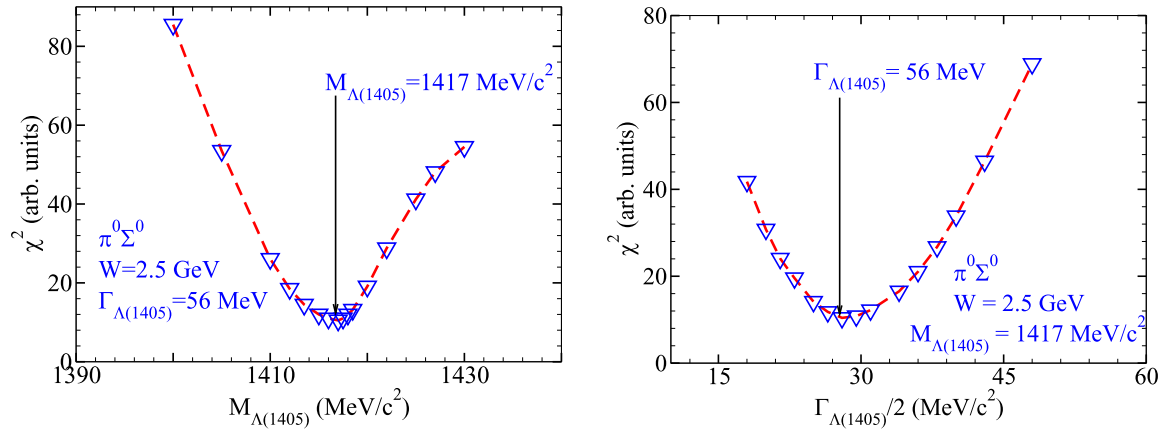

FIG. 6. The dependence of the χ^2 value on the real (left panel) and imaginary (right panel) part of the $\bar{K}N$ pole position. In the left panel, the imaginary part of the pole position is fixed at 28 MeV and the mass of $\Lambda(1405)$ was changed from 1400 to 1430 MeV/c^2. In the right panel, the mass is fixed at 1417 MeV/c^2 and the width was changed from 30 to 100 MeV.

inclusion of relativistic effects will also be important and the relativistic corrections can change the results extracted in the present paper.

IV. CONCLUSION

In the present calculations, we solved the Faddeev AGS equations for the $K\bar{K}N$ system. The $\pi\Sigma$ invariant mass was calculated for all combinations of charges, i.e., $\pi^-\Sigma^+$, $\pi^+\Sigma^-$, and $\pi^0\Sigma^0$ based on this approach. To study the dependence of the $\pi\Sigma$ mass spectrum on the two-body interactions, different types of $\bar{K}N$ and $K\bar{K}$ interactions were used. We calculated the χ^2 value for all models of interaction. It was shown that the mass spectrum resulting from the one-pole version of the $\bar{K}N$-$\pi\Sigma$ potential is in better agreement with the experimental results for the $\gamma p \to K^+(\pi\Sigma)^0$ reaction. However, the extracted results do not confidently say which model of interaction can exactly describe the structure of the $\Lambda(1405)$ resonance.

In the present study, the effect of different factors on the final $\pi\Sigma$ mass spectrum was studied. By solving the full coupled-channel Faddeev equations for the $K\bar{K}N$-$K\pi\Sigma$-$\pi\pi N$-$\pi\eta N$ system, the dependence of the mass spectrum on $t_{\pi\Sigma\leftarrow\pi\Sigma}$ was studied. The effect of different initial channels on the mass spectrum and χ^2 values was investigated and it was shown that, in an exact study of CLAS data, one should consider the effect of these factors. We also used the $\Lambda(1405)$ pole position and width as fitting parameters and, as shown in Fig. 6, a minimum was observed at around $M_{\Lambda(1405)} = 1417$ MeV/c^2 and $\Gamma_{\Lambda(1405)} = 56$ MeV in the χ^2 distribution.

ACKNOWLEDGMENTS

The authors would like to thank the University of Isfahan for the support of the postdoctoral project of the first author (Contract No 136/99).

[1] R. H. Dalitz and S. F. Tuan, Phys. Rev. Lett. **2**, 425 (1959).
[2] R. H. Dalitz and S. F. Tuan, Ann. Phys. (NY) **10**, 307 (1960).
[3] M. H. Alston *et al.*, Phys. Rev. Lett. **6**, 698 (1961).
[4] O. Braun *et al.*, Nucl. Phys. B **129**, 1 (1977).
[5] D. W. Thomas *et al.*, Nucl. Phys. B **56**, 15 (1973).
[6] N. Kaiser, P. B. Siegel, and W. Weise, Nucl. Phys. A **594**, 325 (1995).
[7] E. Oset and A. Ramos, Nucl. Phys. A **635**, 99 (1998).
[8] J. A. Oller and U.-G. Meißner, Phys. Lett. B **500**, 263 (2001).
[9] E. Oset, A. Ramos, and C. Bennhold, Phys. Lett. B **527**, 99 (2002).
[10] Y. Akaishi and T. Yamazaki, Phys. Rev. C **65**, 044005 (2002).
[11] T. Yamazaki and Y. Akaishi, Phys. Lett. B **535**, 70 (2002).
[12] D. Jido, J. A. Oller, E. Oset, A. Ramos, and U.-G. Meißner, Nucl. Phys. A **725**, 181 (2003).
[13] A. Dote, H. Horiuchi, Y. Akaishi, and T. Yamazaki, Phys. Rev. C **70**, 044313 (2004).
[14] T. Hyodo and W. Weise, Phys. Rev. C **77**, 035204 (2008).
[15] J. Esmaili, Y. Akaishi, and T. Yamazaki, Phys. Lett. B **686**, 23 (2010).
[16] J. Esmaili, Y. Akaishi, and T. Yamazaki, Phys. Rev. C **83**, 055207 (2011).
[17] N. V. Shevchenko, Phys. Rev. C **85**, 034001 (2012).
[18] N. V. Shevchenko, Nucl. Phys. A **890-891**, 50 (2012).
[19] J. Esmaili, S. Marri, M. Raeisi, and A. Naderi Beni, Eur. Phys. J. A **57**, 120 (2021).
[20] K. Moriya (CLAS Collaboration) *et al.*, Phys. Rev. C **87**, 035206 (2013).
[21] K. Moriya (CLAS Collaboration) *et al.*, Phys. Rev. C **88**, 045201 (2013).
[22] J. K. Ahn (LEPS Collaboration) *et al.*, Nucl. Phys. A **721**, C715 (2003).
[23] M. Niiyama *et al.*, Phys. Rev. C **78**, 035202 (2008).
[24] J. Siebenson, L. Fabbietti, A. Schmah, and E. Epple, PoS **BORMIO2010**, 052 (2010).
[25] H. Noumi, J-PARC proposal E31; see http://j-parc.jp/NuclPart/Proposal_e.html
[26] C. Curceanu and J. Zmeskal, arXiv:1104.1926.
[27] D. Jido, E. Oset, and T. Sekihara, Eur. Phys. J. A **42**, 257 (2009).
[28] K. Miyagawa and J. Haidenbauer, Phys. Rev. C **85**, 065201 (2012).
[29] D. Jido, E. Oset, and T. Sekihara, Eur. Phys. J. A **49**, 95 (2013).
[30] J. Yamagata-Sekihara, T. Sekihara, and D. Jido, Prog. Theor. Exp. Phys. **2013**, 43D02 (2013).
[31] S. Ohnishi, Y. Ikeda, T. Hyodo, and W. Weise, Phys. Rev. C **93**, 025207 (2016).
[32] K. Moriya (CLAS Collaboration) *et al.*, Phys. Rev. Lett. **112**, 082004 (2014).
[33] L. Roca and E. Oset, Phys. Rev. C **87**, 055201 (2013).
[34] L. Roca and E. Oset, Phys. Rev. C **88**, 055206 (2013).
[35] S. X. Nakamura and D. Jido, Prog. Theor. Exp. Phys. **2014**, 23D01 (2014).
[36] M. Mai and U.-G. Meißner, Eur. Phys. J. A **51**, 30 (2015).
[37] U.-G. Meißner and T. Hyodo, Chin. Phys. C **38**, 090001 (2014).
[38] K. S. Myint, Y. Akaishi, M. Hassanvand, and T. Yamazaki, arXiv:1804.08240v1.
[39] E. O. Alt, P. Grassberger, and W. Sandhas, Phys. Rev. C **1**, 85 (1970).
[40] S. Marri and J. Esmaili, Eur. Phys. J. A **55**, 43 (2019).
[41] S. Marri, S. Z. Kalantari, and J. Esmaili, Chin. Phys. C **43**, 064101 (2019).
[42] S. Marri, Phys. Rev. C **102**, 015202 (2020).
[43] S. Ohnishi, Y. Ikeda, H. Kamano, and T. Sato, Phys. Rev. C **88**, 025204 (2013).
[44] C. B. Dover and G. E. Walker, Phys. Rep. **89**, 1 (1982).
[45] O. Dumbrajs *et al.*, Nucl. Phys. B **216**, 277 (1983).
[46] D. Jido and Y. Kanada-En'yo, Phys. Rev. C **78**, 035203 (2008).
[47] V. Baru *et al.*, Phys. Lett. B **586**, 53 (2004).
[48] L. Schlessinger, Phys. Rev. **167**, 1411 (1968).
[49] H. Kamada, Y. Koike, and W. Gloeckle, Prog. Theor. Phys. **109**, 869 (2003).
[50] V. K. Magas, E. Oset, and A. Ramos, Phys. Rev. Lett. **95**, 052301 (2005).
[51] Z.-H. Guo and J. A. Oller, Phys. Rev. C **87**, 035202 (2013).
[52] T. Inoue, E. Oset, and M. J. Vicente Vacas, Phys. Rev. C **65**, 035204 (2002).

[53] J. A. Oller, E. Oset, and J. R. Peláez, Phys. Rev. D **59**, 074001 (1999).
[54] A. Martinez Torres, K. P. Khemchandani, and E. Oset, Phys. Rev. C **79**, 065207 (2009).
[55] A. Martinez Torres and D. Jido, Phys. Rev. C **82**, 038202 (2010).
[56] H. Feshbach, Ann. Phys. (NY) **5**, 357 (1958).
[57] H. Feshbach, Ann. Phys. (NY) **19**, 287 (1962).
[58] H. Feshbach, *Theoretical Nuclear Physics-Nuclear Reaction* (John Wiley, New York, 1992).
[59] M. Bazzi *et al.*, Phys. Lett. B **704**, 113 (2011).
[60] F. Coester, S. C. Pieper, and F. J. D. Serduke, Phys. Rev. C **11**, 1 (1975).
[61] H. Kamada and W. Glöckle, Phys. Rev. Lett. **80**, 2547 (1998).